Effect of furnace design on atomic absorption and emission signals in spectrochemical analysis
by Stephen Richard Lawson

A thesis submitted in partial fulfillment of the requirements for the degree of . . DOCTOR OF PHILOSOPHY in CHEMISTRY
Montana State University
© Copyright by Stephen Richard Lawson (1981)

Abstract:
An examination has been made of several new furnace designs and applications for both atomic absorption and emission. Problems with current furnace designs are analyzed and experimental data from three new alternate designs are presented. These alternate furnace designs were developed specifically to increase the thermal energy available to analyte molecules before they diffused from the optical path.

A two pronged support furnace was developed in which electric current passed across both ends of an 18mm long graphite tube. The tube center, where the sample was placed, heated by thermal conduction from the ends. Thus the analyte vapor always encountered walls hotter than the surface it left as it diffused toward the furnace ends. This heating mode resulted in ten-fold improvements in lead recoveries from some chloride salts compared to the CRA-63 atomizer. The dependence of lead recoveries on interferent/analyte ratios was also established for lead in magnesium chloride solutions.

A double-walled furnace was also examined and compared to the twopronged support furnace. The heating of this furnace was spatially uniform during the atomization of lead and cobalt. Despite this, recoveries for lead and cobalt were equal or superior to those obtained with the two-pronged furnace. Recoveries for lead in ZnSO4, however, were lower in the double-walled design. Possible mechanisms for these differences are discussed.

Studies on a third design which involved switching of heating modes during atomization were initiated. A graphite furnace was held by four supports which were electrically insulated from one another. A switching circuit changed the polarity of two diagonally opposite electrical supports during the atomization cycle. This changes the electric current direction from across both furnace ends to a lengthwise flow. The switching can be varied to occur at any point in the atomization cycle. The furnace design and circuit schematic are presented.

Generation of electric discharges in a constant temperature Woodriff furnace was explored as a means of creating new emission sources. The long, hot graphite tube provides both long residence times and sufficient thermal energy to decompose and atomize even large solid samples. A d.c. arc, radio-frequency discharge and a microwave discharge were studied. The rf plasma appeared to be the most promising route. Evidence is presented which indicates that thermionic emission from the hot graphite walls aids formation and maintenance of a plasma.

EFFECT OF FURNACE DESIGN ON ATOMIC

ABSORPTION AND EMISSION SIGNALS

IN SPECTROCHEMICAL ANALYSIS

by

Stephen Richard Lawson

A thesis submitted in partial fulfillment
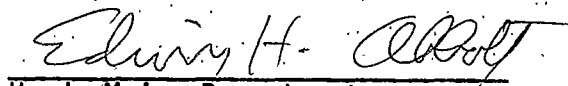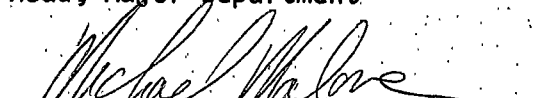of the requirements for the degree

of

DOCTOR OF PHILOSOPHY

in

CHEMISTRY

Approved:

Chairperson, Graduate Committee

Head, Major Department

Graduate Dean

MONTANA STATE UNIVERSITY
Bozeman, Montana

October, 1981

iii

ACKNOWLEDGMENT

TABLE OF CONTENTS

TABLE OF CONTENTS

vi

LIST OF TABLES

vii

LIST OF FIGURES

LIST OF FIGURES

ABSTRACT

An examination has been made of several new furnace designs and applications for both atomic absorption and emission. Problems with current furnace designs are analyzed and experimental data from three new alternate designs are presented. These alternate furnace designs were developed specifically to increase the thermal energy available to analyte molecules before they diffused from the optical path.

A two pronged support furnace was developed in which electric current passed across both ends of an 18mm long graphite tube. The tube center, where the sample was placed, heated by thermal conduction from the ends. Thus the analyte vapor always encountered walls hotter than the surface it left as it diffused toward the furnace ends. This heating mode resulted in ten-fold improvements in lead recoveries from some chloride salts compared to the CRA-63 atomizer. The dependence of lead recoveries on interferent/analyte ratios was also established for lead in magnesium chloride solutions.

A double-walled furnace was also examined and compared to the two-pronged support furnace. The heating of this furnace was spatially uniform during the atomization of lead and cobalt. Despite this, recoveries for lead and cobalt were equal or superior to those obtained with the two-pronged furnace. Recoveries for lead in $ZnSO_4$, however, were lower in the double-walled design. Possible mechanisms for these differences are discussed.

Studies on a third design which involved switching of heating modes during atomization were initiated. A graphite furnace was held by four supports which were electrically insulated from one another. A switching circuit changed the polarity of two diagonally opposite electrical supports during the atomization cycle. This changes the electric current direction from across both furnace ends to a lengthwise flow. The switching can be varied to occur at any point in the atomization cycle. The furnace design and circuit schematic are presented.

Generation of electric discharges in a constant temperature Woodriff furnace was explored as a means of creating new emission sources. The long, hot graphite tube provides both long residence times and sufficient thermal energy to decompose and atomize even large solid samples. A d.c. arc, radio-frequency discharge and a microwave discharge were studied. The rf plasma appeared to be the most promising route. Evidence is presented which indicates that thermionic emission from the hot graphite walls aids formation and maintenance of a plasma.

CHAPTER I

INTRODUCTION

Furnace Designs for Atomic Absorption Spectroscopy

1.   Parameters Influencing Atomic Absorption Analysis

Electrothermal atomizers for atomic absorption spectroscopy have increased considerably since their analytical use was first proposed and studied by L'vov (1) and Woodriff (2). This growth was most pronounced after the introduction of several commercial pulse-heated models in the late 1960's and early 1970's. The individual models and their characteristics will be reviewed later. The furnaces which have evolved during this time are all designed to vaporize and ultimately atomize the sample elements to be determined into a relatively small volume compared to flame techniques (3). The higher gas phase analyte concentrations and longer residence times produced by furnaces result in greater sensitivities and correspondingly lower limits of detection than is attainable with flame atomization. However, the magnitude of furnace sensitivities and the accuracy of a determination are dependent upon the chosen furnace design. This is because the rate of analyte supply into the light path must at least be equal to its rate of removal to achieve the greatest sensitivities (1). The absorbance peak area must also be independent of the sample chemistry for a given amount of analyte. These requirements are not always attained in many

present-day furnace designs (3,4). This is partially due to the needs
for simplicity of operation, compactness, component reliability,
minimal development and fabrication costs, etc. which commercial pro-
duction requires. Thus research among several groups including ours
has concentrated on alternative furnace designs during the last five
years (5-11) in an attempt to meet all the above requirements.

1.1 The Temporal Characteristics of an Absorption Peak

The shape of an absorbance peak generated in any furnace is the
result of two basic time constants: T_1; the time to transfer all the
analyte atoms present into the analytical volume (atomization time) and
T_2; the mean length of time spent by an atom within the light path
(residence time). Both time constants are determined and altered by
parameters of the atomizer design such as heating rate, furnace length,
pressure, heating mode (pulsed or constant), inert gas flow, temporal
and spatial temperature distribution and physico-chemical properties of
the furnace material. i.e. tantalum, molybdenum, tungsten, graphite
(ordinary or pyrolytic), vitreous carbon, etc. The sample matrix
chemistry can also profoundly alter the atomization time (12,13). The
relative importance of these parameters in the various designs avail-
able will be considered in detail later.

The accurate measurement of T_1 and T_2 from experimental
absorption curves should be emphasized. The mathematical model

developed by L'vov (14) defines $\mathcal{T}_1$ as the time elapsed from the moment atomization begins to the point where N_t, the total number of atoms of the analyte within the analytical volume at any time, t, is a maximum. Since the model assumes that the decay of the absorbance signal is independent of the atomization process and atom loss is due to diffusion only, $\mathcal{T}_2$ can be defined from:

$$N_t \geq \mathcal{T}_1 = N_{\mathcal{T}_1} \exp (\mathcal{T}_1 - t)/\mathcal{T}_2 \quad (1.1)$$

where, $N_{\mathcal{T}_1}$, the number of atoms in the analytical volume at the peak maximum is equal to:

$$N_{\mathcal{T}_1} = 2 N_0 \, \mathcal{T}_2^2/\mathcal{T}_1^2 \quad (\mathcal{T}_1/\mathcal{T}_2 - 1) + \exp (-\mathcal{T}_1/\mathcal{T}_2) \quad (1.2)$$

Thus, from this model, the time required for the absorbance signal to increase from the first detectable absorbance to the peak maximum can be used to obtain $\mathcal{T}_1$. $\mathcal{T}_2$ can be calculated from the slope of a log A_0/A_t versus time plot. However, the assumptions of this model ($\mathcal{T}_2 \geq \mathcal{T}_1$) are seldom attained in pulse-heated furnaces. Only the constant temperature furnaces of L'vov and Woodriff have sufficiently long residence times to prevent loss of atoms from the analytical volume before atomization is complete. Even for these furnaces, the model does not account for diffusion complicated by carbide formation. Woodriff, et. al. (15) developed a more thorough model to account for those elements which react with the graphite walls. For such cases,

two time constants are required:

$$M_t = M_0 C \exp(-t/T_a) + M_0 (1-c) \exp(-t/T_b) \qquad (1.3)$$

where M_t is the mass of analyte vapor at time, t, M_0 is the initial weight of analyte, t is the time elapsed after the sample is vaporized, T_a and T_b are time constants which depend upon the graphite (T_2) and gas phase (T_1) diffusion time constants respectively and the equilibrium constant for analyte distribution between graphite and the gas phase. C, the concentration of analyte in the graphite walls, is a function of the equilibrium constant, K, time, wall thickness, (a), tube diameter (x), tube length (1) and Z (Z = x + a).

$$C = BK \sin((\pi Z/a)(T_2/T_a)^{\frac{1}{2}}) \sin(n\pi x/1) \exp(-t/T_a) \qquad (1.4)$$

The decay portion of the absorbance curve can be accurately described by this model even when analyte - wall reactions are present. The two time constants, T_a and T_b, can thereby be obtained from this portion of the curve.

Interpretation of the absorbance curves generated from small, pulse-heated furances is more complicated. Fuller (16) used a simple two-exponential model to describe the rate of atomization and loss of copper atoms from a Perkin-Elmer HGA-70 graphite furnace:

$$\text{Absorbance (Cu)} = k_1/(k_2-k_1)\, p\, [Cu]_0\, (\exp(-k_1 t) - \exp(-k_2 t)) \qquad (1.5)$$

where k_1 is the rate constant of atomization, k_2 is the rate constant

of atom removal and p is a temperature dependent constant which relates the measured abosrbance to the number of copper atoms in the furnace. k_1 was evaluated by plotting log absorbance against time and obtaining k_1 from the slope. Enough copper was deposited in the furance to ensure constant temperature conditions were attained well before complete atomization had occurred. k_2 was then obtained mathematically by a method of successive approximations. An important conclusion resulting from his work was that the rate of atom loss was 3-20 times the rate of atomization depending on the temperature. These measurements were conducted under standard operating conditions for the HGA-70. i.e. an internal gas flow through the furnace of argon. The forced flow removal of atoms from this furnace assures that the majority of absorbance peak shape is determined by the atomization process alone.

An excellent study by Broek and de Galan (4) confirmed the findings of Fuller on the HGA furnace and drew a similar conclusion for the Varian CRA-63 minifurnace. They developed a model to describe the time dependence of the atom population in a furnace using a convolution of a supply function S(t) and removal function R(t):

$$N(t) = \int_0^t S(t') R(t-t') dt' \qquad (1.6)$$

where N(t) is the atom number at time, t, and R(t) is the normalized response when an infinitely rapid atom pulse is supplied. The time constant of the supply function is defined as:

$$\mathcal{T}_s = \int_0^{\infty} S(t) \, dt / S_{max} = No / S_{max} \qquad (1.7)$$

If S(t) is slow in comparison to R(t) (which was confirmed valid experimentally) then T_s can be obtained from the normalized peak area:

$$\mathcal{T}_s = \frac{\int_0^{t} A(t) \, dt}{A_{max}} \qquad (1.8)$$

However, experimentally, one must verify that the removal function is indeed sufficiently rapid to obtain an accurate $\mathcal{T}_s$. Broek and de Galan did this by forcing a high flow (0.5 to 2.0 l/min) of inert gas through the furnace. The peak height continuously decreased as the flow rate increases but the peak shape then represents the supply function. Using silver, lead and manganese, atomizing temperatures between 1000 and 2000K and heating rates between 0.1 and 1.0K/ms, they concluded that $\mathcal{T}_s$ is about 1s in both the CRA-63 and HGA-72 furnaces. They also found the supply function is determined by the furnace temperature and the activation energy and frequency factor of the dominate atom forming process on the furnace surface. This is in agreement with work by Torsi and Tessari (17-19) who used an open graphite rod and Sturgeon, et. al. (20) who used an HGA-2100 furnace. However, the supply function could not be completely modeled by a simple first order Arrhenius - type rate constant. This also agrees with the work of Torsi and Tessari (19). The experimental absorbance curves always exhibited a prolonged tailing compared to the theoretical supply functions.

Broek and de Galan suggested this effect was due to unequal absorption site energies which held the analyte in the graphite matrix until sufficient heat was applied. Gas-phase reactions such as dissociation of dimers and adsorption - redesorption along the furnace wall were considered as possible secondary atom supplies. The high flow rates through the furnaces, however, should have minimized such sources. The fact that experimental - theoretical agreement was better for all three cases (silver, lead and manganese) in the CRA-63 than the HGA-72 suggests the pyrolytic coating on the CRA-63, which reduces solution soaking into the furnace walls, is the cause of the reduced tailing observed in this furnace.

The removal function, $R(t)$, is described by a combination of three transport processes: diffusion, expansion and convection. Approximation of the three processes by an exponential decay allows the net response function to be written as a simple exponential:

$$R(t) = N(t)/N(t_0) = N(t_0) \exp(-t/\tau_R) \qquad (1.9)$$

Experimental measurement of T_R from the absorbance curve requires $S(t) \geqslant R(t)$. Since atomization from the furnace wall was too slow for this purpose, an alternate experiment was carried out. Mercury vapor was rapidly injected into the furnace using an injection syring at varying times during the atomization cycle. The sample could thereby be introduced in less than 10 ms. The time constant, τ_s, was thus

obtained as the slope of a log absorbance as time plot. Once $\mathcal{T}_s$ and its dependence on temperature and heating rate was found, comparison to mathematical descriptions of diffusive, expansive and convective time constants allowed an estimation of the relative contribution each process to the overall removal function.

The time constant for diffusion can be expressed by:

$$\mathcal{T}d = \frac{0.125L^2}{D} \quad (1.10)$$

where L is the furance length in centimeters and D is the mass diffusivity of the analyte in cm^2/sec. For comparison, $\mathcal{T}d$ for a length of 0.9 cm (CRA-63) and D = 1.8 cm^2/sec. is equal to 56 ms while $\mathcal{T}d$ = 544 ms for a 2.8 cm furnace (HGA-72).

The time constant due to expansion of the gas phase as the furnace temperature increases during atomization can be approximated by:

$$\mathcal{T}e = T(t_0)/(dT/dt)_{to} \quad (1.11)$$

where $T(t_0)$ and $(dT/dt)_{to}$ are the temperature and heating rate of the gas at the moment, t_0, that a particular atom is introduced. For a temperature of 1000K and a heating rate of 1K/ms, $\mathcal{T}e$ = 1s.

For larger furnaces like the HGA-72 where a constant internal flow of inert gas induces convective loss of vapor, a third time constant, $\mathcal{T}_c$, must be considered:

$$\mathcal{T}_c = K (V/F) (300/T) \quad (1.12)$$

where F is the cold gas flow rate, V is the cell volume, T is the furnace temperature and K is a proportionality factor dependent on the flow pattern through the furnace. The authors found K difficult to estimate but felt $\mathcal{T}_c$ = 50-100 ms for V equal to a few cm^3, F = 1l/min and T = 1000K.

Experimentally, $\mathcal{T}_R$ was between 100 and 30 ms for mercury in a CRA-63 furnace which led the authors to conclude that diffusion was the dominant removal process in this furnace.

The HGA-72 furnace operated under forced convection conditions had removal time constants between 90 and 150 ms for temperatures between 2500 and 500K respectively indicating forced convection as the dominant removal process. Although these times are longer than Broek and de Galan predicted from equation (1.10), they argue that the flow of argon through the furnace is uncertain. It enters through holes drilled in the wall so that some unknown fraction of the total measured flow flushes the furance vapors. A fraction of 0.5 would account for the difference between experiment and theory. Another possible cause is the gas-wall temperature (up to several hundred K (21)) lag created by the flowing gas. However, this has been reduced in later HGA models by introducing the gas from the furnace ends rather than the center (21).

When operating under static conditions (i.e. stop flow), the removal function of the HGA is dominated by both diffusive and

expansive time constants. At lower temperatures (i.e. 800-1300K) expansion and diffusion are fairly comparable process for atom removal although diffusion tends to be faster. However, at higher temperatures and heating rates, diffusion increases faster than expansion and removal becomes dominated by the diffusion process. The net time constant, T_R, varied between 1.00 and 1.96 s for temperatures and heating rates between 2300K (1.25K/ms) and 800K (1.15/ms) respectively.

In the above model, no element-specific losses such as recombination in the gas phase (22), diffusion through the graphite walls (15), intercalation or carbide formation (15), and condensation at the cooler furnace ends (20,23) were considered. Since the theoretical model used overestimated the observed removal rates, this was apparently justified for the specific cases studied. The authors noted that elements were chosen which minimized such possibilities. However, in general chemical losses must be considered. Formation of carbides, and reactions with the sample matrix to form monochloride, monocyanides, sulfides, etc. can, in some cases, dominate the removal process. In addition, Sturgeon and Chakrabarti (24) were able to demonstrate that the major loss of analyte at atmospheric pressure in the HGA-2100 was diffusion to the cooled furnace ends where condensation occurred. Mercury was detected on the quartz end windows, their brass receptacles and graphite cones following atomization of mercury in the furnace.

However, if no significant revaporization occurred, this finding would not be in conflict with the model of Broek and de Galan.

1.2   Chemical Reactions

1.2.1   Influence of the Furnace Surface

The chemistry of both the furnace and the sample matrix can have a strong influence on the recorded absorbance trace. In fact, either the furnace itself or more commonly, the furnace surface is sometimes altered to reduce matrix interferences. The range of possible materials which are suitable for electrothermal atomizers is fairly limited. Those with sufficiently high melting points and chemical inertness include metal oxides, metals and some allotropes of carbon.

Several metal oxides have been studied in our laboratory because of an interest in using furnaces which were stable toward oxidizing, inert and reducing atmospheres in connection with MHD (magnetohydrodynamics) potassium vapor pressure studies in a constant temperature furnace (24). Beryllium oxide is a good ceramic but is unstable in the presence of water vapor above 1500K (25) and too toxic to be considered. Thorium oxide, although the highest melting of the ceramic oxides (3600K) (26) and very inert to metals at high temperatures, is radioactive and expensive and therefore not practical. Zirconium oxide tubes cracked when heated due to inadequate resistance to thermal stress (24).

Metals were more useful than ceramics as choices for furnace materials. A platinum - rhodium alloy (10% Rh) was very useful for the

MHD work since temperatures above 2069 K were not required. The addition of rhodium increases the hardness and doubles the electrical resistivity of the furnace tube (27). It is sufficiently inert toward oxidizing atmospheres to be run in air and water vapor at elevated constant temperatures. Unfortunately, the limited temperature range and high cost limit its use outside special applications.

Tungsten has the highest melting point (3710K) of all metals and a low thermal coefficient of expansion (26). It is useful for the determination of high boiling, carbide-forming metals. However, its high electrical conductivity, poor machinability and low stability to oxidizing atmospheres limit its use. Tungsten tubes can be run in a hydrogen atmosphere but tend to become brittle with age.

Tantalum (M.P. 3296K) and molybdenum (M.P. 2917K) (26) have been the metals most frequently used as atomizers. Both should be operated in reducing atmospheres. Thus, except for the tantalum strip (28), the majority of work utilizing these metals has been as linings or coatings inside graphite furnaces. L'vov used tantalum foil to line a graphite furnace to prevent diffusion through the walls (3). Fuller found that the rate of copper atomization in a tantalum lined furnace was greater than atomization from a graphite furnace (16). He concluded that the rate-determining step, reduction of copper oxide, was more rapid using tantalum due to the greater free energy change. Henn

(29) decreased interferences on selenium in industrial effluent samples by adding a molybdenum solution to an HGA-2100 furnace. Apparently molybdenum binds to the selenium which allows ashing up to $1700^\circ K$ without loss of analyte. Hodges (30) used orthophosphoric acid as a matrix modifier to prevent interferences on lead in urine samples. However, excessive molecular background resulted from this treatment. Alkali metal chlorides were converted to the corresponding phosphates which lead to the molecular absorption during atomization. He discovered that a molybdenum coating (or more likely Mo_2C) on a graphite furnace significantly reduced this background by the Mo or Mo_2C catalyzed reduction of alkali metal phosphates to phosphides which absorb in the far UV. Zatka (31) soaked HGA-74 furnaces in a 6% tantalum solution to form a uniform layer of TaC (MP 4270K) (26) over the entire furnace. The purpose was to increase the overall inertness of the furnace to oxidative attack. He concluded that, except for carbide formation, possible interferences remained the same as those encountered in untreated graphite furnaces. Stiefel, et. al. (32) coated an HGA-72 furnace with a ZrC layer to obtain increases in sensitivity for beryllium determinations in digested biological tissue. The ZrC layer probably inhibits the formation of Be_2C since greater signal enhancement were obtained for beryllium in aqueous extracts than for benzene solutions. Apparently carbonaceous residues remaining after the dry

and ash cycles of benzene solutions resulted in beryllium carbide for-. mation. Lanthanum solutions were used to coat furnaces for lead analyses in non-saline waters (33) and fertilizers (34). Thompson, et. al. suggested that the LaC_2 surface may cause a shift in the appearance temperature of lead. Such a shift can decrease the temporal overlap between analyte and interfering salts thereby increasing recovery (35). Sturgeon et. al. (20), concluded that atomic lead is formed by reduction of the oxide to the metal by graphite then subsequent vaporization into the gas phase. However, in the absence of reducing agents, $PbO_{(s)}$ sublimes to $PbO_{(g)}$ (36) which lends support to the above hypothesis.

All of the furnace materials and coatings mentioned thus far suffer from a reduced range of general application compared to furnaces coated with pyrolytic graphite. While a metal carbide layer may reduce formation of analyte carbides, the furnace is no longer useful for the determination of the element used for the coating or any other elements which may be present as trace impurities in the coat. Pyrolytic graphite layers are easily grown on a graphite surface by the pyrolysis of methane in argon at $\sim$ 1400 K (37). Sturgeon and Chakrabarti (38) have presented a thorough review of the properties of graphite and pyrolytic graphite. It should be stressed here, however, that pyrolytic graphite provides the impermeability and inertness to carbide

formation and oxidation for which metal carbides have been used buy

without the disadvantages. For those situations where the carbide

layer was used to modify the sample matrix to prevent interferences, we

argue that a correct furnace design using pyrolytic graphite would

obviate such a need. By a correct design we are referring to atomi-

zation into an isothermal environment, sufficiently high temperatures

for complete atomization and long residence times (i.e. $T_2 \geq T_1$).

Vitreous (or glassy) carbon is also a possible material for fur-

naces. It has graphite - like sheets in layers with some SP^3 bonding

between layers and an overall more amorphous structure than graphite

(39). This results in a 3-8 times greater electrical resistance than

graphite but it is also 6-7 harder (40). It has about the same gas

permeability as hard glass. Although inert to oxidation and most

carbide forming metals, it is readily attacked by alkali metals (41).

However, it can be heated in air up to 900 K without weight loss (24).

Studies in this lab on 15 cm long furnace tubes in a constant tempera-

ture furnace found vitreous carbon tubes had a lifetime twice that of

a pyrolytically coated graphite tube at 2300K (24). Thus vitreous

carbon appears to be the superior furnace material. Unfortunately, it

is expensive, difficult to machine due to its hardness (W_2C or diamond

drills) and has a slightly higher coefficient of thermal expansion than

graphite. Cups of vitreous carbon shattered when rapidly heated in a

CRA-63 atomizer. The spring tension on the supports required to maintain good electrical contact was too large for the cup during heating. In general, pyrolytic graphite is equally effective at a lower cost and can be produced in the lab for any shape part with simple apparatus.

1.2.2 Analyte - Matrix Interactions

Ideally, variations in the chemical composition among different samples will have no effect on the integrated absorbance measured for a given amount of analyte and therefore aqueous solutions of simple metal salts can be used to calibrate the AA system. However, as most AA users have discovered, this is often not the case. In fact, in many commercial labs, results are not considered reliable unless the method of standard additions has been applied. Considering the number of matrix interferences reported in the literature such an approach is certainly reasonable. However, caution is advised when using this method since studies conducted in this lab on the Pb-$MgCl_2$ system demonstrated that the degree of signal supression can be dependent on the matrix/analyte ratio (7). Lead recoveries obtained for $MgCl_2$/Pb ratios less than 2000 varied substantially with increasing amounts of lead. Obviously, standard additions would not be useful in this situation, but at ratios of 2500 to 10,000, lead recoveries are constant for a fixed amount of magnesium chloride (Table 5).

The sample matrix can affect the atomization process in three

ways: (1) A change in the appearance temperature of the analyte. This can be due to a change in the chemical form in which the analyte is bound on the furnace surface relative to the calibration standard. The change in temperature therefore reflects a change in the activation energy, E_a, of the atomization process (20). The earlier appearance temperature can also be caused by the "carrier distillation effect" often observed and utilized in emission spectroscopy (42, 43). In this case, all or part of the matrix carries the analyte into the gas phase as it volatilizes. Entry of analyte into the gas phase at lower temperatures can result in loss of analyte in molecular form due to insufficient temperatures for atomization. (2) Higher or lower appearance temperatures can also result in increased or decreased atomization rates. Changes in atomization rates can also be due to a change in the rate determining step of atomization or a shift in the equilibrium involved in the atomization process. (3) The matrix can bond to the analyte on the atomizer surface or in the gas phase. Analyte thereby leaves the optical path in molecular form causing an absorbance decrease. The most widely reported interferences of this type are due to the formation of metal monochlorides (44,45), monocyanides (46), and sulfides (47).

Matrix interferences can be suppressed by two means: (1) Alteration of the analyte-matrix chemistry. This can be accomplished by a

wide variety of methods (29-36). The particular choice often being

dependent on both the analyte to be determined and the chemical compo-

sition of the sample. This restrictive applicability hinders the

practical utilization of multielement AAS to complex samples when such

methods are employed. However, they can be effective for limited

situations. The use of metal carbide or pyrolytic graphite coatings on

the furnace covered in the previous section (1.2.1) is one class of

pre-treatments which reduce interferences. The resulting inert layer

forms a physical barrier between the analyte and the underlying

graphite. Matrix-generated carbonaceous material can still form car-

bides but generally to a lesser degree. (2) The more widely encounter-

ed pre-treatments involve addition of reagents which change the

molecular form in which the analyte is bound (29,30,48-50) and/or form

a strong bond to the interfering anion (35,44,52). Reagents such as

orthophosphoric acid (30,48-50) and molybdenum salts (29,48) form

compounds with the analyte which are less volatile than the original

form (e.g., chloride salts). A higher ashing temperature can thereby

be used to volatilize the interfering matrix without loss of analyte.

Chloride salts can be removed at lower ashing temperatures by adding

ascorbic acid (53-55). oxalic acid (53) or hydrogen gas (51) prior to

or during the ash stage. The chloride is thereby bound as HCl which is

easily vaporized. This technique has been especially useful for the

determination of lead which can be lost as the volatile chloride at
ashing temperatures below 900K (51). The mechanism by which ascorbic
and oxalic acids reduce interferences on Pb, Mn, Cu and Co from sea-
water and other matrices is still uncertain. Regan and Warren (54)
proposed that pyrolysis of ascorbic acid left a carbon residue which
aided in the reduction of analyte oxides during the atomization step.
However, Hydes (53) obtained the same improvements in Cu sensitivity
using oxalic acid which does not leave a carbon residue. Although
McLaren and Wheeler (55) showed that ascorbic acid changed the type of
lead oxide formed when lead nitrate was pyrolyzed from red litharge to
thermally unstable massicot, the mechanism does not account for sensi-
tivity improvements obtained for other elements using this reagent.
Early atomization of lead as a less stable oxide may decrease the
analyte - matrix temporal overlap but loss of significant amounts of
chloride as HCl gas during asking probably plays the dominate role in
reducing interferences. Another effect proposed by Hydes (53) may also
contribute to the observed improvements. He noticed that the surface
tension of the sample drop was reduced when the ascorbic or oxalic
acid was added. No visible salt crystals remained after drying al-
though they were observable in the absence of the acids. The improved
thermal contact between sample and furnace created by the finer salt
crystals may accelerate decomposition of the matrix. Recent experiments

by Kahn, et. al. (10) using an autosampler on an IL555 furnace provide support for this mechanism. Interferences on lead and gold were reduced by simply aspirating a solution of the sample through a pneumatic nebulizer and spraying the resulting aerosol into the furnace which is preheated to approximately 450K. The solution dries on contact and leaves a uniform layer of very fine crystals on the graphite surface. The authors suggested that this technique prevented interferences associated with solutions soaking into the porous graphite and those caused by formation of large crystals during sample drying (52). However, the technique also reduced gas phase interferences (e.g., chloride interferences). This suggests that a change in heat transfer to the sample and/or a change in the physical contact between sample and the graphite surface caused by this uniform layer of fine crystals reduces the formation of analyte compounds during the atomization cycle. Thus the physical nature of the dried sample can also exert an influence upon the measured atomic absorbance signal. It would be interesting to compare these results with those from similar experiments run on a furnace coated with pyrolytic graphite or tantalum. This would provide a qualitative measure of the importance of surface/sample contact changes to the observed interference reductions.

The use of hydrogen in the sheath gas during ashing and atomization has been demonstrated to be an effective means of eliminating the

interference from chloride salts on lead. French and Cedergren (51) compared the magnitude of interferences on lead in steel samples dissolved in hydrochloric and nitric acids when analyzed in both the CRA-63 and HGA-72 furnaces. They found that the HGA-72, because it was constructed of ordinary graphite, produced enough hydrogen from traces of water left after the drying stage to remove all the chlorine present (as $FeCl_2$) and thus prevent an interference on lead. The CRA-63, which is constructed of pyrolytic graphite, generates five times less hydrogen during the ashing stage than the HGA-72. Insufficient amounts of chlorine were removed to prevent interferences. However, addition of hydrogen to the argon gas which shields the graphite parts from oxygen eliminated the remaining chlorine provided an ashing temperature of at least 775K was utilized. An optimum ashing temperature between 900 and 1000K was required for the HGA-72 because of the smaller amount of hydrogen present.

Strong acids remove interferences from halide salts by a mechanism similar to hydrogen (35,52). Phosphoric, sulfuric and nitric acid all helped to remove chlorine through formation and vaporization of HCl in the ashing step. However, the volatility and anion of the acid were also important. Phosphoric and sulfuric acid were more effective in eliminating interferences on lead and nickel from copper chloride than nitric acid. Phosphoric and sulfuric acid are also less volatile and

form pyrophosphates and sulfates of the interferents. Thus sufficient acid is present at elevated temperatures to react with the chloride salt. The pyrophosphate and sulfate salts have very low molecular absorbances and therefore background absorbance is also reduced.

Finally, we stress the importance of atomizer design as the means of eliminating the influence of chemical reactions on the atomic absorbance signal. Matrix-induced variations in the appearance temperature and/or atomization rate will not affect the integrated absorbance signal if the furnace tube is held at a constant temperature during the entire volatilization and atomization of the sample. A constant temperature eliminates variations in the diffusion and convection rates of atom removal during the absorption pulse. If the furnace is sufficiently long (or the sample sufficiently small) such that $T_2 \gg T_1$, then the absorbance peak will not be affected either. Gas phase interferences are eliminated by providing sufficient thermal energy and residence times to assure complete atomization before any analyte leaves the optical path. Knowledge of the furnace temperature prior to the beginning of volatilization is therefore valuable. When the above conditions have been met, the upper limit of matrix which can be tolerated may then be determined by the background absorbance level. However, to some extent, this too can be minimized using higher atomization temperatures.

1.3 Length, Temperature and Pressure

The relationship of length, temperature and pressure to peak height and peak area has been developed by L'vov (3) for a constant temperature furnace. The conditions of diffusion-controlled atom loss and $T_2 \gg T_1$ are required to prevent forced convection and slow atomization rates from dominating the absorbance peak shape. When these requirements are fulfilled, the absorbance peak height can be expressed as:

$$A_{peak} \simeq (f/AwS \, \Delta \nu_s) \, M \qquad (1.13)$$

and the peak area by:

$$A_{area} \simeq (f \, _2/Aw \, \Delta \nu s) \, M \qquad (1.14)$$

where f is the oscillator strength of the atomic absorption line, T_2 is the mean residence time of an atom in the optical path, Aw is the atomic weight of the element concerned and M its mass in grams, S is the transverse cross-sectional area of the furnace and $\Delta \nu_s$ is the displacement of the frequency maximum of a line relative to its initial position as a result of a change in pressure of a foreign gas and/or temperature. For a furnace operated at atmospheric pressure (eg. the furnace design by Woodriff) the Lorentz contribution to $\Delta \nu_s$ is usually small. The measured absorbance terms can then be expressed by the following furnace parameters:

$$A_{peak} \simeq (T^{0.7}/S) \; M \qquad (1.15)$$

and,

$$A_{area} \simeq (1^2P/ST^{0.9}) \; M \qquad (1.16)$$

Where the temperature dependence of ΔV_s and the temperature and pressure dependence of T_2 has been inserted. Note that peak height does not depend on the furnace length (provided $T_1 \ll T_2$) but only on the cross sectional area. Thus small diameter furnaces are preferable where physical possible (i.e. factors such as light throughput must also be considered). The peak area varies directly with P and the square of the furnace length. Both terms are a result of the T_2 dependence on these parameters:

$$T_2 = 10^3 1^2 P/D_0 T^{1.6} \qquad (1.17)$$

where D_0 is the analyte differsion coefficient at standard conditions (STP). The furnace length is therefore very important for sensitivity, especially relative sensitivity, under these conditions.

The furnace used by L'vov (1) was operated at several atmospheres pressure of argon. The line profile is then governed almost entirely by the Lorentz effect. When the pressure dependance of ΔV_s is added, the absorbance expressions become:

$$A_{peak} \simeq (T^{0.7}/SP) \; M \qquad (1.18)$$

and,

$$A_{area} \simeq (1^2/ST^{0.9}) \; M \qquad (1.19)$$

the peak height now has an inverse dependance on pressure but the pressure dependance of peak area has been eliminated.

For pulsed atomizers, T_2 is usually smaller than T_1. Therefore, heating rate can have a large influence on peak height. Chakrabarti, et. al. demonstrated this influence using capacitive discharge heating of an anisotropic pyrolytic graphite tube (56). The authors expressed the temperature dependance of the rate constant for the evaporation of an analyte element into the analytical volume by an Arrhenius expression:

$$k(T) = A\exp(-\Delta H/RT) \qquad (1.20)$$

where A is a frequency factor, H is the heat of vaporization of the element, R is the gas constant and T is the temperature in degree Kelvin. This equation can also be expressed as a function of time by substituting $T_0 + \alpha t$ for T where T_0 is the furnace temperature immediately before the start of the atomization cycle (usually the temperature at the end of the ash cycle; 500-900K), α is the furnace heating rate in K/ms and t is the time in ms. When $\alpha t \gg T_0$, the rate constant expression becomes:

$$k(t) \sim A\exp(-\Delta H/R\alpha t) \qquad (1.21)$$

When $\alpha t \ll T_0$:

$$k(t) = A\exp(-\Delta H/RT_0) \exp(\Delta H/RT_0^2)\alpha t \qquad (1.22)$$

In either case, k varies exponentially with the heating rate. Since extremely rapid heating rates were used (up to 60K/ms), a steady state temperature was usually reached before the first appearance of atoms in the gas phase. Therefore, assuming first order kinetics and steady state temperatures, k is inversely proportional to the atomization time τ_1. Using L'vov's (14) model for the relation between the analyte population when time $t = \tau_1$ (i.e. the absorbance maximum) and the time constants τ_1 and τ_2 under accelerated vaporization rates:

$$N_{peak} = 2N_0 \tau_2^2/\tau_1^2 (\tau_1/\tau_2 - 1 + \exp(-\tau_1/\tau_2)) \qquad (1.23)$$

where N_0 is the total number of analyte atoms and N peak the number at $t = \tau_1$, one can see that the absorbance maximum will increase exponentially with the heating rate, α, since τ_1 decreased exponentially with k and α. It is also assumed that τ_2 remains constant with increasing α. This valid as long as a steady state temperature is reached before the first appearance of analyte atoms in the gas phase. When heating rates become sufficiently large to satisfy the condition, $\tau_2 \gg \tau_1$, then

$$N_{peak} = N_0 \qquad (1.24)$$

and L'vov's model for temperature, length and pressure influences on absorbance peak height and peak area apply. Sensitivity enhancements up to 27-fold were observed using capacitive discharge heating (56).

2. Designs of Commercial Pulse - Heated Electrothermal Atomizers

2.1 Massmann and HGA Atomizers

The pulse-heated furnace originally introduced by Massmann (57)
was 55 mm long, and 6.5 mm internal diameter. Electrical contact was
made at both ends. The tube center, which contained the sample, heated
first and remained hotter than the ends by several hundred degrees
throughout the atomization cycle. The Perkin - Elmer Corp. adopted the
Massmann design for commercial production and use. The first model,
HGA-72, 2000, had a larger internal diameter, 8.6 mm, but a similar
length, 53 mm. Removable quartz lenses fitted as windows of the fur-
nace housing and capped both ends of the furnace tube. The furnace was
therefore semienclosed with ports to allow a flow of argon or nitrogen
to shield the graphite furnace parts. Part of this flow flushed the
internal portion of the furance. This internal purge gas flowed from
the sample port at the center to the ends and its magnitude was a fixed
fraction of the total gas flow.

This design had several drawbacks. (1) The large internal dia-
meter results in lower peak height and peak area sensitivities because
of the larger cross sectional area which is inversely proportional to
both methods of measuring sensitivity (44). Larger diameters are also
more difficult to fully illuminate with the light source which can de-
crease the integrated absorbance more than the peak maximum. (2)

Large gas-wall temperature differences have been observed for this

furnace (up to several hundred degrees) (58,59) and the later HGA-2100

model (60). This was the result of both the large internal diameter

of the furnace (which was decreased to 6 mm in the HGA-2100) and the

internal purge gas. Broek, et. al. (21) concluded that in the absence

of internal gas flow (stopped-flow conditions) this temperature differ-

ence was at most 100K. They also concluded that preheating the gas

before entering the furnace would also significantly reduce this pro-

blem. (3) L'vov (44) compared theoretical estimates of sensitivities

for the HGA-2100 to experimental values measured by Sturgeon, et. al.

(60). He found good agreement only for elements of low volatility

(Cd, Sn and Zn). The sensitivities obtained for Cu, Mo and V were

less than one third of the predicted values. L'vov attributed the

poor correlation to the non-uniform temperature distribution along the

furnace length. Findlay et. al. (61) recorded a temperature of 600K

at the ends of an HGA-2000 when the center was only 1100K. Low

volatility elements condense at the furnace ends where they are re-

evaporated very slowly or not at all. As a result, the effective

length of the furnace is decreased which decreases the residence time

($T_2 \propto \ell^2$). Long, broad tailing of the absorption pulse was observed

for the HGA furnace which was not apparent for the uniformly heated

CRA-63 (62). This drawn out tailing was difficult to fully integrate

and therefore part of the absorption pulse was left unrecorded. (4) The power applied to the furnace tube was determined by that required to maintain the final temperature. This sets an upper limit on the heating rate and therefore prevents optimization of peak absorbance sensitivity. Higher applied power increases the heating rate but also results in higher temperatures during the absorbance pulse. Consequently, the diffusivity increases and lowers the average residence time, T_2. Sturgeon et. al. (60) found that the integrated absorbance decreased with higher atomization temperatures except for elements which were difficult to atomize (eg. Al and Cu). This can be explained by the equivalence of T_1 and T_2 observed for most elements under the stopped-flow conditions used by the authors. The decreases in T_2 are more important and although peak absorbance initially increases with temperature, further increases cause a decline in both peak and integrated absorbance. However, for those elements for which $T_1 \gg T_2$ initially, increases in atomization temperature increase both peak and integrated absorbance. The decrease in T_1 continually increases the gas phase atom concentration faster than lower T_2 values can decrease it.

All of the above disadvantages have been solved with varying degrees of success over the last decade. The HGA-2200 model has been reduced in size to a 6 mm internal diameter and 28 mm length. The

internal purge gas flows from the ends toward the center at a rate
independent of the external gas sheath. This substantially reduces the
gas-wall temperature difference during atomization. Electronic valves
have also been added to shut off the purge gas during atomization which
increases T_2 and also lowers the gas-wall temperature difference. A
temperature feedback loop utilizing a photodiode has been added to
allow variation of the heating rate independent of the final atomization
temperature reached. The power level is automatically reduced
when a predetermined temperature has been reached. The increased
heating rates now available result in improved peak and integrated
absorbances particularly for the more refractory metals. Some inter-
ferences are also reduced by the faster heating because the condition
$T_2 \gg T_1$ is more nearly fulfilled than in earlier models. The HGA-
2100 and HGA-2200 models are also pyrolytically coated to prevent
carbide formation and diffusion through the walls. Slavin et. al.
(63) solved the problem of non-uniform heating along the furnace length
with a contoured tube. The ends of a conventional HGA-2200 tube were
tapered so that they heated slightly faster than the center. This
reduced the temperature difference between the center and ends from
1000K to 100K when the center temperature was 2800K. Unfortunately,
up to 50% more power was required to heat the contoured tube. The
center heated more slowly than in the conventional tube which resulted

in lower peak absorbances for some elements. No improvements were obtained for elements like vanadium which had produced absorbances far below theoretical in the conventional design.

2.2 CRA Atomizers

The CRA model atomizers were developed by Varian Techtron, Inc. in the early 1970's. They are the smallest tubular electrothermal atomizers in commercial use. The original CRA-61 model had an inside diameter of only 1.5 mm and a length of 4.5 mm. The small diameter was excellent for sensitivities in terms of atom density however the full potential of such a low cross sectional area was lost by the small T_2 values resulting from the short length. Focusing of the light source also became a problem with such a small diameter. Therefore, when the length was increased to 9 mm in the CRA-63, the diameter was also widened to 3 mm. Both models were relatively open furnaces. Electrical contact was made at the tube center by two pyrolytically coated graphite support rods. The furnace itself was also constructed of pyrolytically coated graphite. The graphite parts were protected from atmospheric oxygen by a flow of nitrogen or argon moving upwards from rows of corrugated steel located directly below the furnace. This small, compact system does not suffer from the non-uniform temperature distribution and gas-wall temperature differences which plagued the earlier HGA models. The principal disadvantage of these atomizers is

the short residence times ($\sim$20 - 100 ms) compared to the relatively

long atomization times ($\sim$1 sec) (4). Sturgeon et. al. (60, 62) per-

formed a thorough comparison of the CRA-63 and HGA-2100 atomizers.

The average of sensitivities obtained for three elements (Cd, Sn and Zn)

in each furnace revealed the HGA-2100 produced 3.3 times larger peak

absorbance values than the CRA-63 but only 0.6 times the integrated

absorbance value. Both values agreed well with the theoretical esti-

mates of L'vov: 4.0 and 0.40 respectively (44). The large difference

in peak absorbances reflects the difference in T_2 values (about a

factor of 10 larger in the HGA-2100). A much smaller fraction of the

total analyte atoms occupy the CRA-63 furnace at any moment compared

to the HGA. However, the larger integrated absorbances in the CRA

are a result of the higher atom densities created by its smaller cross

sectional area.

The larger T_1/T_2 ratios observed in the CRA furnaces also affect

the manner in which increasing atomization temperatures alter the peak

and integrated absorbances. The power applied to the CRA-61 and CRA-

63 furnaces was also, like the HGA-2000 and HGA-2100, determined by the

required final temperature. However, unlike the HGA furnaces, increas-

ing the final atomization temperature resulted in steadily increasing

peak absorbances while the integrated absorbance remained unchanged

(62). Since only 5-10% of the analyte atoms introduced are contained

in the furnace at the absorbance maximum (4), substantial increases in the heating rates would be required before the peak absorbance decreased. Apparently, the decreases in T_2 caused by the higher temperatures offsets the increases in peak absorbance so that integrated absorbance remains unchanged. Although the effect of higher atomization temperatures is not as deleterious in the CRA's as in the HGA furnaces, peak and integrated abosrbance would increase if heating rates were independent of the final temperature.

The major changes incorporated into the latest model, the CRA-90, have been the addition of a temperature feedback control circuit and an optional hydrogen diffusion flame which is part of the sheath gas. The advantages of ashing and atomizing in the presence of hydrogen gas were covered earlier. The addition of this feature has significantly increased the amounts of chloride salts which can be tolerated in a sample without interference.

Several parameters characteristic of both the CRA and HGA furnaces are summarized in Table 1.

2.3 The IL-455 and IL-555 Atomizers

A more recent manufacturer of electrothermal atomizers for AA is Instrumentation Laboratory, Inc.. Their furnace is growing in popularity and have some features which deserve mention. Both the IL-455 and IL-555 furnaces are constructed of pyrolytically coated graphite with

dimensions of 4.5 mm inside diameter and a 38 mm length. Thus these furnaces have an average residence time greater than either the CRA or HGA furnaces and a cross sectional area intermediate between them. Theoretically, the IL furnaces should have the highest sensitivities among the three types of atomizers considered. Table 1 lists the sensitivities for five elements in each furnace. Except for cadmium, the IL has better sensitivities.

Electrical contact is made at both ends of the furnace and the center heats first as in the CRA and HGA models. However, no detailed measurements have been reported on any temperature non-uniformity or its effects. The IL-555 is equipped with a temperature feedback control circuit utilizing a tungsten resistance thermometer to decouple the heating rate from the final atomization temperature.

Two features on the IL-555 which are unique to commercial electrothermal atomizers are the Fastac auto-sampling system and a pressurized atomization chamber. The Fastac auto-sampler was mentioned briefly in section 1.2.2 and will be discussed in detail in the next section. Pressurization is achieved by enclosing the furnace in a chamber with an automatic or manually controlled access door. Pressures up to four atmospheres argon are possible. The principal advantage of pressurization is the resulting increase in residence time. Thus $T_2 \gg T_1$ may be attained although this has not been

Table 1

Characteristic Parameters for Three Pulse-Heated Commercial Atomizers

Atomizer	Inner Diam. (mm)	Length (mm)	(ms)	S^a (cm^{-2})	Q/N_2^b (s/cm^2)	Experimental Sensitivities ^{c}				
						Cd	Cu	V	Sn	Mo
HGA-2100	6	28	200	.29	0.7	3.5E-13	2.1E-11	4.0E-10	2.9E-10	8.8E-11
CRA-63	3	9	20	.071	.28	9.5E-14	2.7E-12	3.1E-11	9.1E-12	7.5E-12
IL-555	4.75	38	361	.18	2.0	4E-13	8E-13	1/5E-11	6E-12	6E-12

a: $S = d^2/4$, where d is the furnace diameter in cm.
b: $Q/N = /S$ is the theoretical peak area sensitivity.
c: Weight in grams of element which gives a peak absorbance of 0.0044.

36

documented in the literature. This would eliminate interferences arising from matrix-induced changes in T_1 and improve precision.

3. Alternate Designs for Pulse-Heated Electrothermal Atomizers

The remainder of this chapter is devoted to recent changes in pulse-heated furnaces designed specifically for the elimination of matrix-induced alterations in peak and integrated absorbances. The most difficult interference to remove has been the formation of gas-phase analyte molecules which leave the furnace volume before decomposing to atoms. This is the result of inadequate heat transfer to the analyte species during its residence in the furnace. However, this is unavoidable with the furnace designs just mentioned. When the sample is deposited on a cold furnace wall then heated at the low rates now used, (0.1 - 2.0K/ms) thermodynamically stable analyte molecules are formed and vaporized as the temperature is scanned across their volatilization range. In the case of lead in a chloride salt matrix, the time required to reach the atomization temperature is important in determining the distribution of lead among various lead compounds (45). The most recent changes in atomizer design have therefore been made to increase the heating rate, increase heat transfer rates or subject the analyte vapors to temperatures higher than the surface they left before leaving the furnace.

3.1 The L'vov Platform

L'vov, Pelieva and Sharnopolsky (64) first proposed the use of a graphite platform installed inside a furnace from which samples were vaporized rather than the furnace wall. This delayed vaporization until the furnace wall was somewhat hotter than the platform. The magnitude of this difference depended on the heating rate of the wall and the rate of heat transfer to the platform. As a means of minimizing heating due to heat conduction from the furnace walls, the platform was constructed of anisotropic pyrolytic graphite due to its low heat conductivity in the direction perpendicular to the plane of deposition. The platform was a rectangular plate 4 mm x 5 mm and 1 mm thick with sections along two opposite edges cut out to reduce contact with the walls. The platform slid into an HGA-2100 furnace which was operated in the usual manner except that longer drying times were necessary. The peak absorbances of high volatility elements were shifted to higher furnace temperatures more than low volatility elements. Peak heights were increased an average of 1.5 times when high and mid-volatility elements were vaporized from the platform whereas no increase was observed for low volatility elements. L'vov (44) explained these results as a consequence of the more rapid heating rate of the platform compared to the rate of change of the wall temperature. Since part of the platform heating is due to radiation from the walls, its heating

rate is proportional to the fourth power of the wall temperature:

$$\frac{dT_p}{dt} \propto T_w^4 - T_p^4 \qquad (2.1)$$

where T_p is the platform temperature and T_w is the wall temperature. For low volatility elements, the temperature difference between platform and wall becomes so small that the platform heating rate is that of the wall. Therefore no changes in peak height are observed

Slavin and Manning (65,55) studied the effects of the platform on matrix interferences. They modified the platform by placing a depression in the center to allow use of larger sample volumes (up to 50 $\mu\ell$). An HGA-2200 was used to allow temperature control during the atomization stage by means of the temperature feedback circuit. Interferences on Cu, Mn, Cd, Pb and Tl from chloride, phosphate and sulfate salts were also reduced using the platform. Twenty times more NaCl could be tolerated when determining lead with the platform than without. When the temperatures of the wall and platform had equilibrated, a temperature difference between wall and platform of $\sim 150^{\circ}C$ was present when the wall was at $2050^{\circ}C$.

3.2 Capacitive Discharge Heating

L'vov also first suggested the use of a condenser bank as a large energy source to perform the initial heating of a furnace up to the final temperature (44). After that, a low output power supply could